

## Supplementary Information for

### Neutrophil and natural killer cell imbalances prevent muscle stem cell mediated regeneration following murine volumetric muscle loss

Jacqueline A. Larouche<sup>1,2</sup>, Paula M. Fraczek<sup>1,2</sup>, Sarah J. Kurpiers<sup>1</sup>, Benjamin A. Yang<sup>1,2</sup>, Carol Davis<sup>3</sup>, Jesus A. Castor-Macias<sup>1,2</sup>, Kaitlyn Sabin<sup>1,2</sup>, Shannon Anderson<sup>4</sup>, Julia Harrer<sup>4</sup>, Matthew Hall<sup>1</sup>, Susan V. Brooks<sup>1,3</sup>, Young C. Jang<sup>4,5</sup>, Nick Willett<sup>6</sup>, Lonnie D. Shea<sup>1</sup>, Carlos A. Aguilar<sup>1,2,7\*</sup>

<sup>1</sup>Dept. of Biomedical Engineering, University of Michigan, Ann Arbor, MI 48109, USA.

<sup>2</sup>Biointerfaces Institute, University of Michigan, Ann Arbor, MI 48109, USA. <sup>3</sup>Department of Molecular & Integrative Physiology, University of Michigan, Ann Arbor, MI 48109, USA.

<sup>4</sup>Department of Biomedical Engineering, Georgia Institute of Technology and Emory University, Atlanta, GA 30332, USA <sup>5</sup>School of Biological Sciences, Georgia Institute of Technology, Atlanta, GA 30332. <sup>6</sup>University of Oregon, Eugene, OR 97403, USA <sup>7</sup>Program in Cellular and Molecular Biology, University of Michigan, Ann Arbor, MI 48109, USA.

\*To whom correspondence should be addressed: [caguilar@umich.edu](mailto:caguilar@umich.edu)

#### This PDF file includes:

Supplementary methods  
Supplementary references  
Figures S1 to S8

## Supplementary Methods Text

**Animals:** C57BL/6 wild-type female and male mice were obtained from Jackson Laboratories or a breeding colony at the University of Michigan (UM). Pax7Cre<sup>ER/+</sup>;Rosa26<sup>mTmG/+</sup> (mTnG) and Pax7Cre<sup>ER/+</sup>;Rosa26<sup>dTomato/+</sup> mice were obtained from a breeding colony at UM and administered 5 daily 100 $\mu$ L intraperitoneal injections of 20mg/mL tamoxifen in corn oil. All mice were fed normal chow ad libitum and housed on a 12:12 hour light-dark cycle under UM veterinary staff supervision. All procedures were approved by the University Committee on the Use and Care of Animals at UM and the Institutional Animal Care and Committee and were in accordance with the U.S. National Institute of Health (NIH).

**Injury Model:** Adult mice (3-4 months) were anesthetized with 1.5% isoflurane and administered 0.1mg/kg buprenorphine in 100 $\mu$ L saline. Puralube ointment was applied to both eyes to prevent dryness. Hair was removed from the hindlimbs using clippers, followed by Nair hair removal cream. The surgical area was wiped with Providone Iodine followed by 70% ethanol three times to sterilize. A 1cm incision was made in the skin on the anterior side of each quadriceps, followed by the removal of a 2mm or 3mm full depth muscle section from middle of the rectus femoris muscle. In tissues used for histological and immunohistological analysis, a suture was placed in the muscle to identify the middle of the injury. No intramuscular sutures were placed in tissues used for flow cytometry or scRNA-Seq due to the foreign body response induced around the suture. The skin was sutured closed using 7-0 proline sutures, which were removed 7 days post-surgery.

## Histology

**Tissue Sectioning:** Quadriceps muscles from both hindlimbs were embedded in optical cutting temperature (OCT) compound and frozen right after excision in isopentane previously cooled with liquid nitrogen then stored at -80°C. Ten serial cross sections were cut using a cryotome at -20°C at the suture delineating the midpoint of the injury and collected on positively charged glass slides (Fisher #12-550-15). Duplicate or triplicate cross sections from each timepoint and wound size were placed on the same slide to control for possible staining differences between slides.

**Hematoxylin and Eosin Staining:** Slides were submerged in hematoxylin for two minutes followed by two sets of ten quick immersions in distilled water. Slides were then submerged in Scott's tap water (20.0g magnesium sulfate heptahydrate and 2.0g sodium bicarbonate in 1L tap water) and distilled water for one minute as well as one set of ten immersions in 80% ethanol. After one minute of Eosin immersion slides were immersed ten times in two different 95% ethanol baths and a 100% ethanol bath. Finally, slides were submerged in SafeClear II for one minute, and two drops of Permunt were added before placing the coverslip on top. Brightfield images were taken using a motorized Olympus IX83 microscope at 10X magnification and stitched using the Olympus CellSense software to obtain an image of the complete tissue section.

**Picrosirius Red Staining:** Slides were removed from -80°C, thawed to room temperature, and dried for 30 minutes before fixing in 4% paraformaldehyde in PBS for 15 minutes at room temperature. Following fixation, slides were washed 3 times in PBS for 5 minutes each, 2 times in deionized water for 5 minutes each, allowed to dry for 10 minutes at RT, and incubated in 0.5g Direct Red 80 solubilized in 500mL Picric Acid for 1 hour at room temperature. Next, slides were washed twice with acidified water (2.5mL Glacial Acetic Acid in 500mL deionized water) for 5 minutes each followed by 2 washes in deionized water for 5 minutes each. Tissue samples were then dehydrated in a series of ethanol washes (50%, 70%, 70%, 90%, 100%, 100%), incubated in Xylenes twice for 5 minutes each, and mounted with Permunt. Brightfield images were taken using a motorized Olympus IX83 microscope at 10X magnification and stitched using the Olympus CellSense software to obtain an image of the complete tissue section. Images were converted to RGB stack and converted to greyscale. To calculate collagen fraction, the green channel was automatically thresholded and measured using ImageJ, then divided by the surface area of the tissue section based on thresholding the red channel to include only the tissue. Two or three sections per tissue were stained and quantified, then averaged to get the percentage of collagen for each tissue.

**Immunohistofluorescent Staining:** Immunofluorescence staining was performed as previously reported<sup>1</sup>. Briefly, slides were removed from -80°C, thawed to room temperature for 30 minutes, then fixed in ice-cold 100% acetone at -20°C for 10 minutes. Following fixation, slides were air-dried for 10 minutes at RT, tissue sections were circled with Hydrophobic Barrier PAP Pen and allowed to dry at room temperature. Tissue sections were rehydrated in PBS for 5 minutes at RT, then blocked for 1 hour at room temperature using 10% normal goat serum (NGS) in PBS. After blocking, slides were incubated overnight at 4°C in a solution containing primary antibodies (rabbit anti-laminin (1:500 dilution), goat anti-NKp46/NCR1 (3ug/mL) and/or rat anti-Ly6G (1:500)) diluted in 10% NGS. Primary antibodies were then washed three times for 5 minutes with PBS at room temperature. Secondaries (donkey anti-goat AF488 (1:500 dilution), goat anti-rabbit AF555 (1:500 dilution), goat anti-rat AF647 (1:500), and/or goat anti-mouse AF488 (1:500)) and Hoescht 33342 (1:500 dilution) were added in PBS and incubated for 1 hour at RT. After incubation, slides were washed three times with PBS and a coverslip was mounted using Prolong Diamond fluorescent mounting medium. Slides were allowed to dry overnight, then stored at 4°C until imaging. Images were acquired with a Nikon A1 confocal microscope equipped with Colibri 7 solid state light source and pseudo colored using ImageJ. Myofiber area and Feret diameters were quantified based on stitched images of laminin stains using the MuscleJ<sup>2</sup> plugin for ImageJ and R for plotting.

### **Extraction and Preparation of Single Cell Suspension from Muscle**

Mouse quadriceps were extracted, and separately weighed using sterile surgical tools and placed into separate petri dishes containing ice-cold PBS. Using surgical scissors, muscle tissues were minced and Collagenase type II (0.2%) and Dispase II (2.5U/mL) were added to 10mL of DMEM per quadricep. Samples were placed on rocker in a 37°C incubator for 1 hour and mixed by pipette every 30 minutes. The enzymes within the slurry were then inactivated by addition of 20% heat-inactivated fetal bovine serum (HI-FBS) in Ham's F10 media. The solution was passed through a 70um cell strainers, centrifuged, washed, and counted.

### **Flow Cytometry**

The single cell suspension was pelleted and re-suspended in staining buffer (PBS with 2% BSA, 2mM EDTA and 0.01% sodium azide) at 2E8 cells/mL, then 200uL of cells were plated into round-bottom 96-well plates for staining. Cells were centrifuged at 250xg for 2.5 minutes. The supernatant was discarded and cells were re-suspended in a primary antibody cocktail that included one or more of the following: CD11b-PE (1:200 dilution), CD11b-APC (1:200 dilution), CD45-AF488 (1:100 dilution), CD68-FITC (1:400 dilution), APC-CD335 (NKp46) (1:40 dilution), Ly-6A/E-APC (1:200), CD45-APC (1:200), Ter119-APC (1:200), CD29-PE (1:100), and/or BV421-Ly6G (1:400 dilution). Cells were incubated in primary antibody for 30 minutes on ice, then centrifuged, washed with staining buffer, then re-suspended in staining buffer containing propidium iodide (1:400 dilution) for 1 minute at room temperature in the dark, centrifuged, and re-suspended in staining buffer for flow cytometry analysis. Prior to acquisition, cells were filtered through 40µm cell strainers to prevent cytometer clogging. Single color controls were made using UltraComp eBeads compensation beads stained according to manufacturer's protocol. Florescent minus one controls were made using a mix of cells from each sample. For analysis of apoptosis, cells were stained with Annexin V immediately prior to flow cytometry analysis according to manufacturer's instructions. Samples were acquired within 1 hour on a BioRad Ze5 cytometer, and the data was processed using FlowJo (version 10) with manual compensation.

### **Real-Time PCR (qRT-PCR)**

Cell lysates were thawed at room temperature for 30 minutes, then RNA was extracted using the Qiagen miRNeasy Micro Kit according to manufacturer's instructions. RNA purity and concentration were measured using a NanoDrop and Qubit RNA HS Assay. Within one week, cDNAs were synthesized using the SuperScript III cDNA Synthesis Kit according to manufacturer's protocol. DNA quality and concentration was determined using a NanoDrop. 80-100ug cDNA template was plated in triplicate along with SYBR Green PCR MasterMix and 500nM PCR primer, then cycled 40 times starting at 95°C for 10 seconds followed by 60°C for 30 seconds on a CFX96 Real-Time thermocycler. Gene expression was quantified using the  $\Delta\Delta C_t$  method.

## NK Cell and Neutrophil Co-Culture

Murine IL15 super agonist (mIL15SA) was complexed as previously described<sup>3</sup>, aliquoted in sterile PBS with 0.1% BSA, and stored at -80°C until use. Splenic NK cells were magnetically enriched from uninjured young WT mice using Miltenyi mouse NK Cell Isolation Kit per manufacturer's instructions and cultured for 48 hours in RPMI containing 10% FBS, 60ng/mL mIL15SA, and antibiotics to activate. NKp46<sup>+</sup> NK cell purity following magnetic enrichment was determined to be >80% by flow cytometry (Supp. Fig. 4b). Neutrophils were FACS-enriched (CD11b+Ly6G+PI-) from mouse skeletal muscle 7 days post 3mm VML injuries. NK cells and neutrophils were co-cultured at a 10:1 ratio for 4 hours at 37°C in RPMI with 10% FBS and antibiotics. Following incubation, cells were stained with Annexin V and PI according to manufacturer's protocol, then immediately analyzed on a BioRad Ze5 flow cytometer. Data was analyzed using FlowJo.

## NK Cell Transplants

Splenic NK cells were obtained as described above and activated in vitro using IL15SA for 48 hours. Activated NK cells were washed and re-suspended in sterile PBS (50K cells/10 $\mu$ L) and transplanted into 3mm and 2mm VML defects 7-dpi using a 29 ½ G needle. Contralateral limbs were used as controls and received PBS only. At 14-dpi, mice were euthanized, and neutrophil abundance was quantified by flow cytometry (CD11b+Ly6G+PI-).

## CCR1 Inhibition

Mice were administered bilateral 3mm VML defects. Starting 7dpi mice received daily IP injections of CCR1 inhibitor J-113863 (8mg/kg) solubilized in sterile PBS with 5% DMSO and 5% CremophorEL. Neutrophil abundance was quantified by flow cytometry (PI<sup>-</sup>CD11b+Ly6G<sup>+</sup>) at 14-dpi.

## TGF $\beta$ RII Inhibition

Mice were administered bilateral 3mm VML defects to the quadriceps, or 2mm VML defects to the tibialis anterior for force testing. Starting 3-dpi mice received intramuscular injections of ITD1 (200pg in 20 $\mu$ L using a 29 ½ G needle) in sterile PBS with 0.01% DMSO every third day until 15-dpi. Contralateral limbs were injected with 20 $\mu$ L of vehicle (PBS with 0.01% DMSO) every third day. Neutrophil abundance was quantified by flow cytometry at 14-dpi, and healing was assessed histologically at 28-dpi as described above.

## Muscle Force Testing

**Quadricep:** Quadriceps strength was determined through a terminal procedure under anesthesia at 8 weeks to measure the peak isometric tetanic torque about the knee. A 2 cm long incision was made to expose the femoral nerve. After isolating the posterior branch of the femoral nerve with a nerve cuff, the mouse was restrained such that the knee was at a 90-degree angle and the ankle is connected to a force transducer (Isometric Transducer Model No. 60-2996, Harvard Apparatus). The nerve was stimulated using a stimulus generator (GRASS S11 Stimulator, Grass Technologies) to induce the contraction of the quadriceps femoris. The pulse duration, frequency, and train duration of the stimulator were set to 0.2ms, 175 Hz, and 500ms respectively. The nerve was stimulated with progressively increasing voltages until the peak isometric tetanic torque was reached. Then maximal torque was recorded three times in a row for consistent force production.

**Tibialis Anterior:** Force testing was performed as previously reported by Dellorusso et al. with some modifications<sup>4</sup>. Mice were anesthetized with 2% Isoflurane to maintain a deep anesthesia throughout the experiment. Hindlimb fur was removed with animal clippers. The TA muscle was exposed by removing the overlying skin and outer fasciae. The distal TA tendon was isolated, and the distal half of the TA was freed from adjacent muscles by carefully cutting fasciae without damaging muscle fibers. A 4-0 silk suture was tied around the distal tendon, and the tendon was severed. The animal was then placed on a temperature-controlled platform warmed to maintain body temperature at 37°C. A 25-gauge needle was driven through the knee and immobilized to prevent the knee from moving. The tendon was tied securely to the lever arm of a servomotor via

the suture ends (6650LR, Cambridge Technology). A continual drip of saline warmed to 37°C was administered to the TA muscle to maintain its temperature. The TA muscle was initially stimulated with 0.2 ms pulses via the peroneal nerve using platinum electrodes. Stimulation voltage and muscle length were adjusted for maximum isometric twitch force (Pt). While held at optimal muscle length (Lo), the muscle was stimulated at increasing frequencies until a maximum force (Po) was reached, typically at 200 Hz, with a one-minute rest period between each tetanic contraction. Subsequently, the same procedure was repeated, but rather than activating the muscle via the peroneal nerve, a cuff electrode was placed around the muscle for stimulation. Muscle length was measured with calipers, based on well-defined anatomical landmarks near the knee and the ankle. Optimum fiber length (Lf) was determined by multiplying Lo by the TA Lf/Lo ratio of 0.6<sup>5</sup>.

After the evaluation of isometric force, the TA muscle was removed from the mouse. The tendon and suture were trimmed from the muscle, and the muscle was weighed. After removal of TA muscles, deeply anesthetized mice were euthanized by the induction of a pneumothorax. Total muscle fiber cross-sectional area (CSA) of TA muscles was calculated by dividing muscle mass by the product of Lf and 1.06 mg/mm<sup>3</sup>, the density of mammalian skeletal muscle<sup>6</sup>. Specific Po was calculated by dividing Po by CSA.

### **Muscle Progenitor Cell Differentiation**

**Primary Cells:** After obtaining a single cell suspension, magnetic enrichment of MuSCs was performed using the mouse Satellite Cell Isolation Kit according to manufacturer's instructions. Meanwhile, a 10cm tissue culture dish was coated with 10% Matrigel in DMEM as previously published<sup>7</sup>. Enriched MuSCs were seeded onto the dish in 8mL myoblast medium (Ham's F10 containing 20% HI-FBS, 10ug/mL fibroblast growth factor (bFGF), and 1X penicillin/streptomycin). Cells were expanded for 5 days with fresh media added every other day. Following expansion, 50,000K cells were passaged using 0.25% trypsin and seeded into each well of a Matrigel-coated 12-well plate and expanded until 90-100% confluency in myoblast media. At this point, myoblast media was replaced with differentiation media (DMEM with 5% horse serum and 1% penicillin/streptomycin) and allowed to differentiate for 72 hours.

**C2C12s:** Mice were humanely euthanized, and PBMCs were collected from the heart into tubes containing 8uL of 0.5M EDTA. Neutrophils were magnetically enriched from PBMC using a mouse Neutrophil Isolation Kit (Miltenyi) according to manufacturer's instructions, then incubated for 48 hours in C2C12 growth media (DMEM with 10% FBS, bFGF, and antibiotics) to generate neutrophil conditioned media. Control conditioned media was generated by incubating C2C12 growth media for 48 hours. Conditioned media was then collected and filtered to remove cell debris. C2C12s were expanded in a 96-well plate for either 8 days or 1 day in C2C12 growth media containing conditioned media, with media replenished every 48 hours. Following expansion, media was replaced with differentiation media and cells were incubated for 72 hours.

**Immunofluorescence Staining:** After 72 hours in differentiation media, myotubes were rinsed twice with PBS, then fixed with 4% paraformaldehyde for 20 minutes at room temperature (RT). After three quick washes with 1X PBS, cells were incubated for 15 minutes at RT with 0.1% TritonX-100, washed three times with 1X PBS, and blocked for 1 hour at RT with 1% BSA, 0.1% Tween-20 and 22.52mg/mL glycine in 1X PBS. After blocking, cells were incubated with primary antibodies (1:10 dilution of anti-MYH3) overnight at 4°C followed by secondary antibodies (1:500 dilution of AF555 anti-rabbit) overnight at 4°C. Following secondary stain, cells were washed three times in 1X PBS, then nuclei were stained with Hoechst 33342 (1:500 dilution). Immunolabeled cells were imaged on a Zeiss epifluorescent microscope using a 20X objective. Ten images were acquired and analyzed per well. The fusion index was automatically calculated using MATLAB as the ratio of nuclei within myofibers containing more than 2 nuclei divided by the total number of nuclei per image. Myonuclei as a percentage of total cells were calculated by hand as the number of MyH3+ myotubes with more than 2 nuclei divided by the total number of cells.

**Real-Time PCR:** After 72 hours in differentiation media, myotubes were rinsed twice with PBS then collected into Qiazol, vortexed for 1 minute, incubated for 5 minutes at room temperature, and stored at -80° until further analysis. qRT-PCR was performed as described above.

### Single-cell mRNA Sequencing

**Sample Preparation and Sequencing:** Freshly isolated cells were briefly stained with Propidium iodide (PI) and FACS sorted to remove dead cells (PI positive) and debris. An equal number of viable cells were pooled from two mice and 10,000-16,000 cells were loaded into the 10x Genomics chromium single cell controller and single cells were captured into nanoliter-scale gel bead-in-emulsions (GEMs). cDNAs were prepared using the single cell 3' Protocol as per manufacturer's instructions and sequenced on a NovaSeq 6000 (Illumina) with 26 bases for read1 and 98x8 bases for read2. Except for 7-dpi, which was repeated twice pooling two mice of the same gender, sequencing libraries were generated from a pool of cells from one male and one female mouse.

**Data Processing and Analysis:** 10x CellRanger v2.0.0 software's mkfastq and count command were run with default parameters except expect-cells=10000. HDF5 matrix files were imported into R (<https://www.r-project.org/>) using the Seurat v3 package<sup>8</sup> and genes expressed in less than 200 cells or cells expressing less than 3 genes were removed. Seurat objects were merged and cells with >10% mitochondrial genes or over 7500 reads were deemed low quality and removed. Following normalization, identification of variable features, and scaling using default parameters, datasets were integrated using Seurat's FindIntegrationAnchors (dims = 1:30, k.filter = 200, k.score = 30, anchor.features = 2000) and IntegrateData functions. Dimensional reduction was performed in Seurat using PCA, then UMAP<sup>9</sup> followed by community detection using the Louvain algorithm (resolution = 0.5). Cluster marker genes were determined both with Seurat (only.pos = T, min.pct = 0.25, logfc.threshold = 0.25, return.thresh = 0.01) and scCATCH (species = 'Mouse', match\_CellMatch = T, tissue = 'Muscle', cell\_min\_pct = 0.25, logfc = 0.25, pvalue = 0.05) to annotate cell types. Defect-associated differential gene expression among celltypes was calculated using MAST<sup>10</sup> as previously reported<sup>11</sup>. NicheNet<sup>12</sup> interaction predictions were generated using the Seurat Wrapper according to the vignette to compare the 3mm (degenerative) defects to the 2mm (regenerative) defects. Trajectory analysis was performed on the myogenic cell clusters using scVelo<sup>13</sup> and the respective Seurat Wrapper. Loom files for were generated using velocity<sup>14</sup>. Seurat and ggplot2 were used for data visualization.

### Statistics

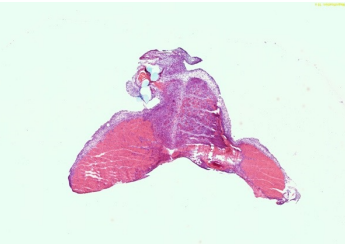
Experiments were repeated at least twice, apart from scRNA-Seq. Bar graphs show mean  $\pm$  standard error unless otherwise stated. Statistical analysis was performed in MATLAB and/or R using two-sample Student's t-test assuming normal distribution and equal variances, one-way ANOVA, paired-T-test, or Kolmogorov-Smirnov test for distributions, as specified in figure captions. All statistical tests performed were two-sided. Outliers were determined using the Tukey's fences method with k = 1.5 and removed from further analysis. P-values less than 0.05 were considered statistically significant. Effect sizes were estimated using Cohen's d.

### Supplementary References

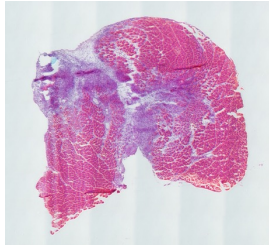
1. Markworth, J. F. *et al.* Resolvin D1 supports skeletal myofiber regeneration via actions on myeloid and muscle stem cells. *JCI Insight* **5**, (2020).
2. Mayeuf-Louchart, A. *et al.* MuscleJ: a high-content analysis method to study skeletal muscle with a new Fiji tool. *Skelet. Muscle* **8**, 25 (2018).
3. Guo, Y. *et al.* IL-15 Superagonist-Mediated Immunotoxicity: Role of NK Cells and IFN- $\gamma$ . *J. Immunol.* **195**, 2353–2364 (2015).
4. Dellorusso, C., Crawford, R. W., Chamberlain, J. S. & Brooks, S. V. Tibialis anterior muscles in mdx mice are highly susceptible to contraction-induced injury. *J. Muscle Res. Cell Motil.* **22**, 467–475 (2001).
5. Burkholder, T. J., Fingado, B., Baron, S. & Lieber, R. L. Relationship between muscle fiber types and sizes and muscle architectural properties in the mouse hindlimb. *J. Morphol.* **221**, 177–190 (1994).

6. Mendez, J. & Keys, A. Density and composition of mammalian muscle. *Metabolism* **9**, 184–188 (1960).
7. Motohashi, N., Asakura, Y. & Asakura, A. Isolation, culture, and transplantation of muscle satellite cells. *J. Vis. Exp.* (2014) doi:10.3791/50846.
8. Butler, A., Hoffman, P., Smibert, P., Papalexi, E. & Satija, R. Integrating single-cell transcriptomic data across different conditions, technologies, and species. *Nat. Biotechnol.* **36**, 411–420 (2018).
9. Becht, E. *et al.* Dimensionality reduction for visualizing single-cell data using UMAP. *Nat. Biotechnol.* **37**, 38–47 (2019).
10. Finak, G. *et al.* MAST: A flexible statistical framework for assessing transcriptional changes and characterizing heterogeneity in single-cell RNA sequencing data. *Genome Biol.* **16**, 278 (2015).
11. Dulken, B. W. *et al.* Single-cell analysis reveals T cell infiltration in old neurogenic niches. *Nature* **571**, 205–210 (2019).
12. Browaeys, R., Saelens, W. & Saeys, Y. NicheNet: modeling intercellular communication by linking ligands to target genes. *Nat. Methods* **17**, 159–162 (2020).
13. Bergen, V., Lange, M., Peidli, S., Wolf, F. A. & Theis, F. J. Generalizing RNA velocity to transient cell states through dynamical modeling. *Nat. Biotechnol.* (2020) doi:10.1038/s41587-020-0591-3.
14. La Manno, G. *et al.* RNA velocity of single cells. *Nature* vol. 560 494–498 (2018).

3mm 7 days



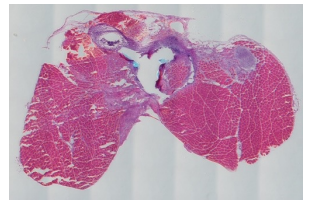
3mm 14 days



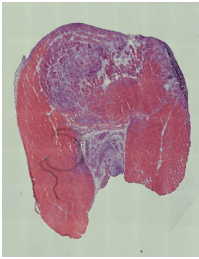
3mm 28 days



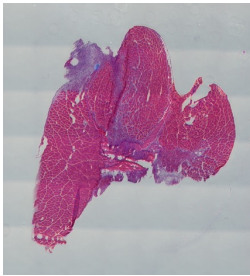
3mm 42 days



2mm 7 days



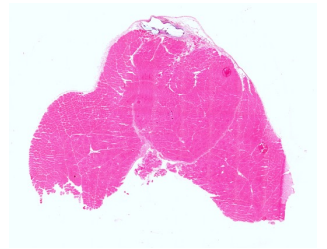
2mm 14 days



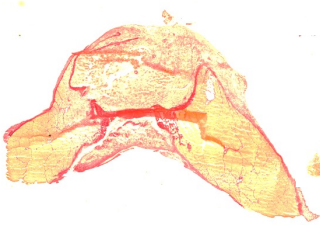
2mm 28 days



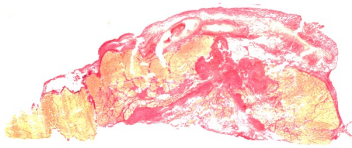
2mm 42 days



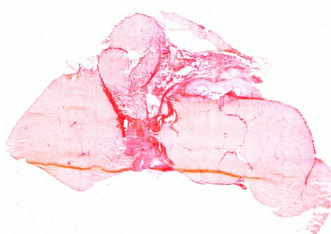
3mm 7 days



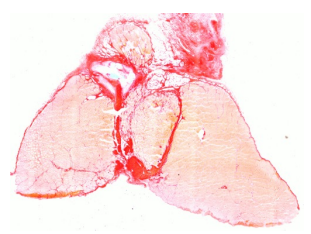
3mm 14 days



3mm 28 days



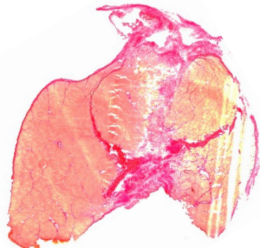
3mm 42 days



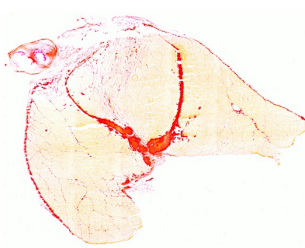
2mm 7 days



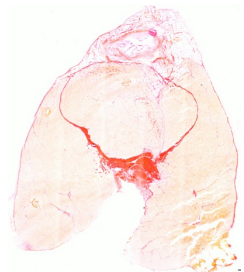
2mm 14 days



2mm 28 days

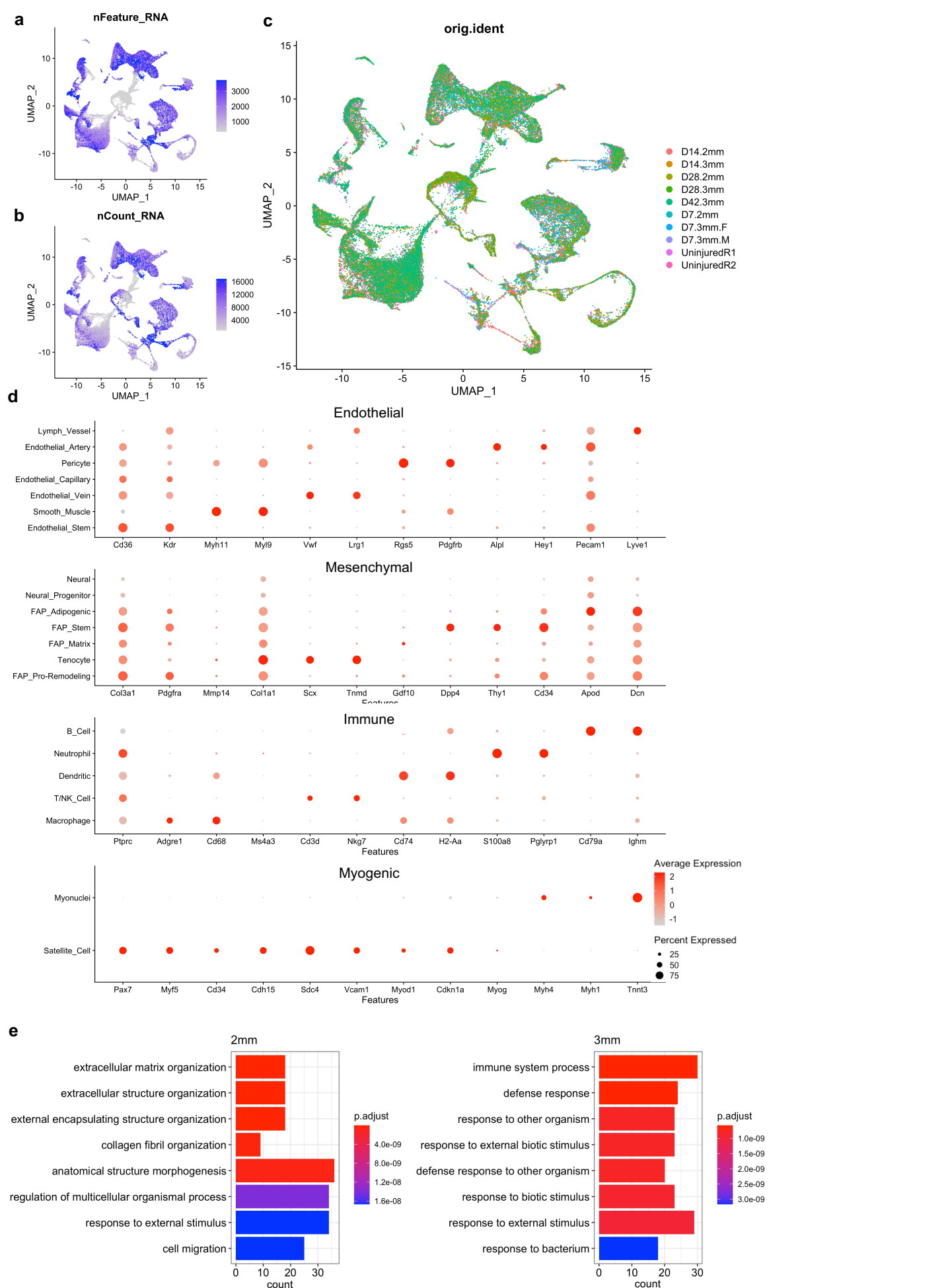


2mm 42 days

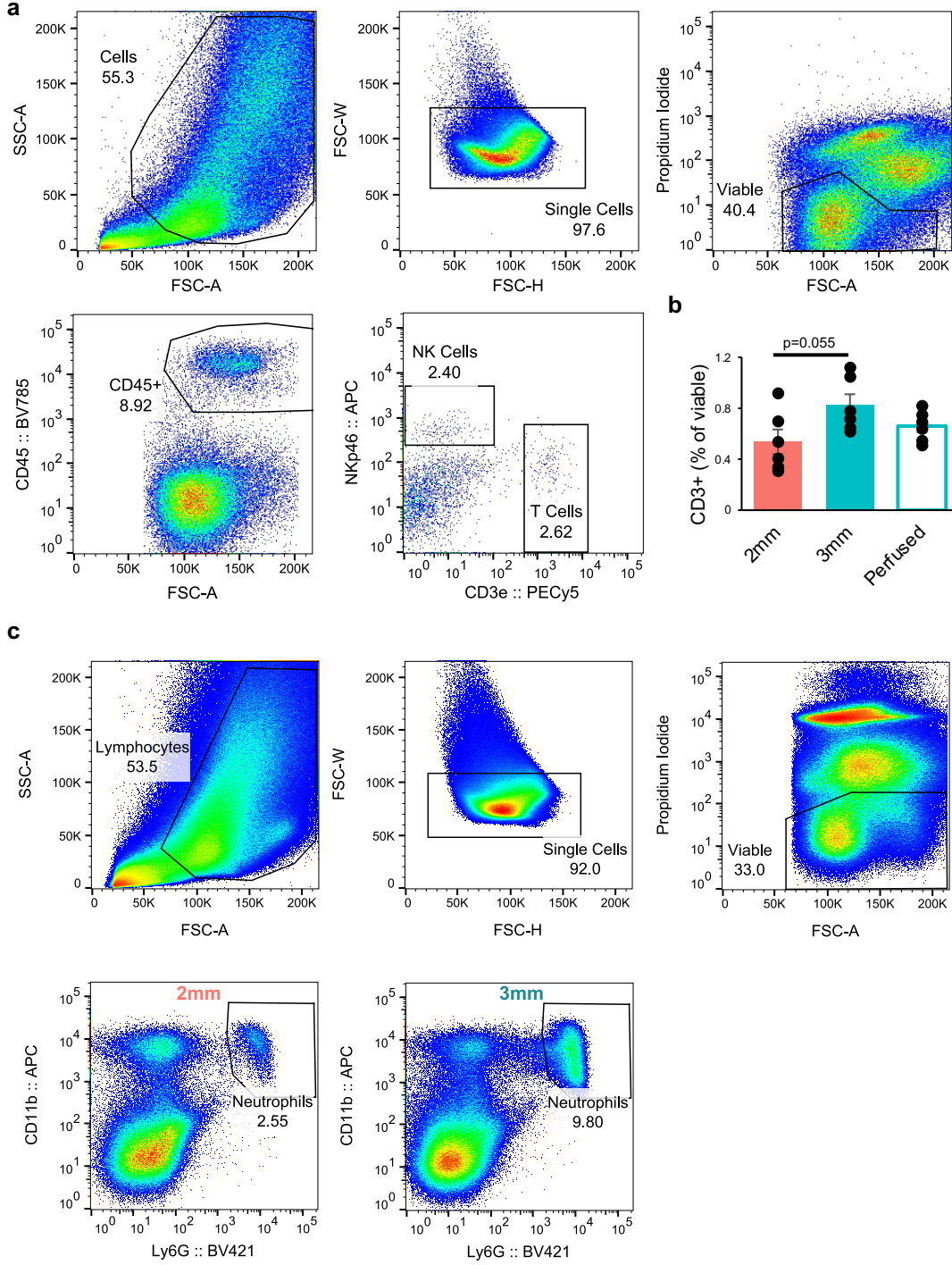


**Supplemental Figure 1. Representative images of quadriceps after regenerative (2mm) and degenerative (3mm) volumetric muscle injuries isolated at different time points. Representative full section images of H&E (top two rows) and PSR (bottom two rows) stained tissues.**

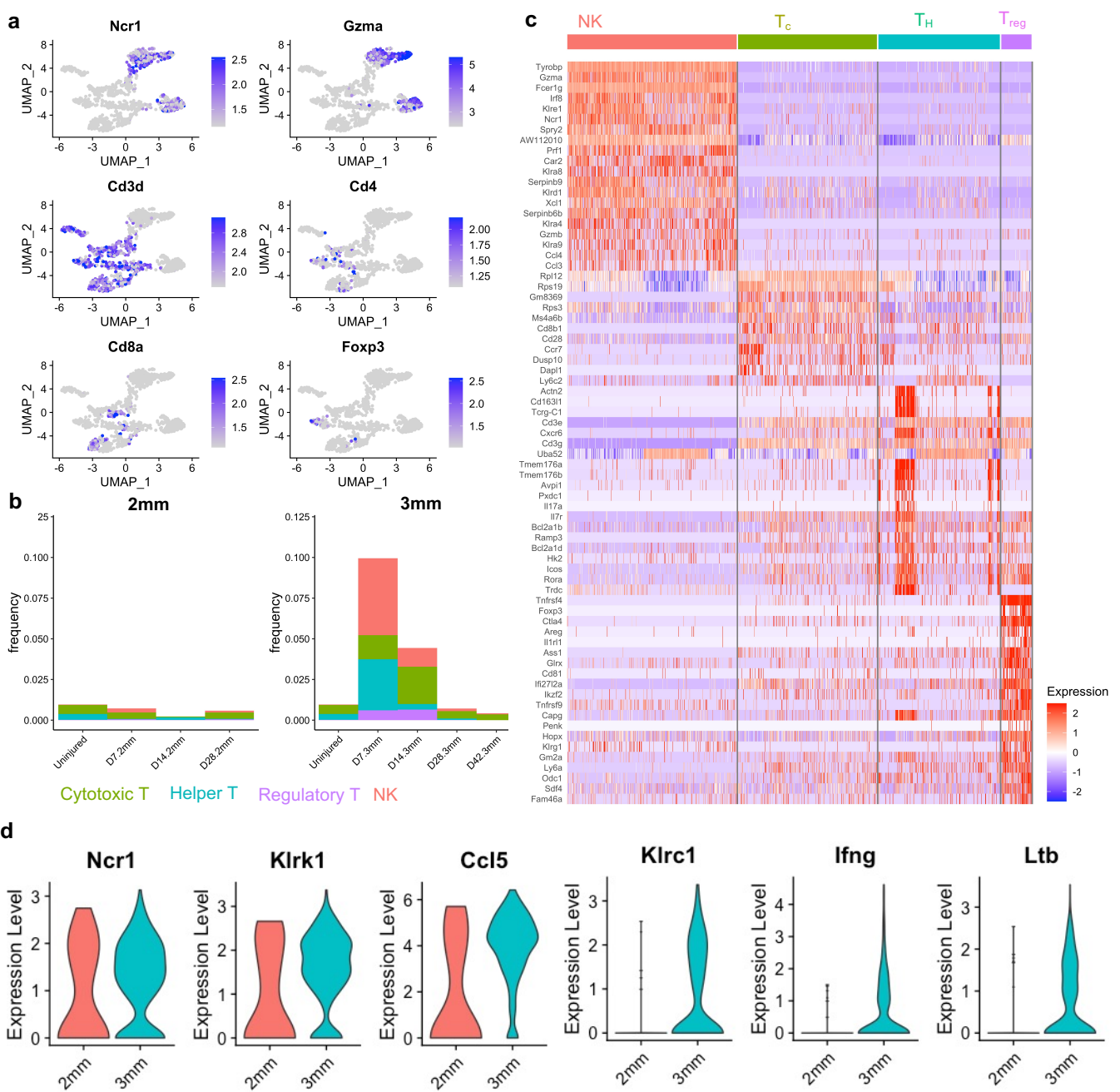




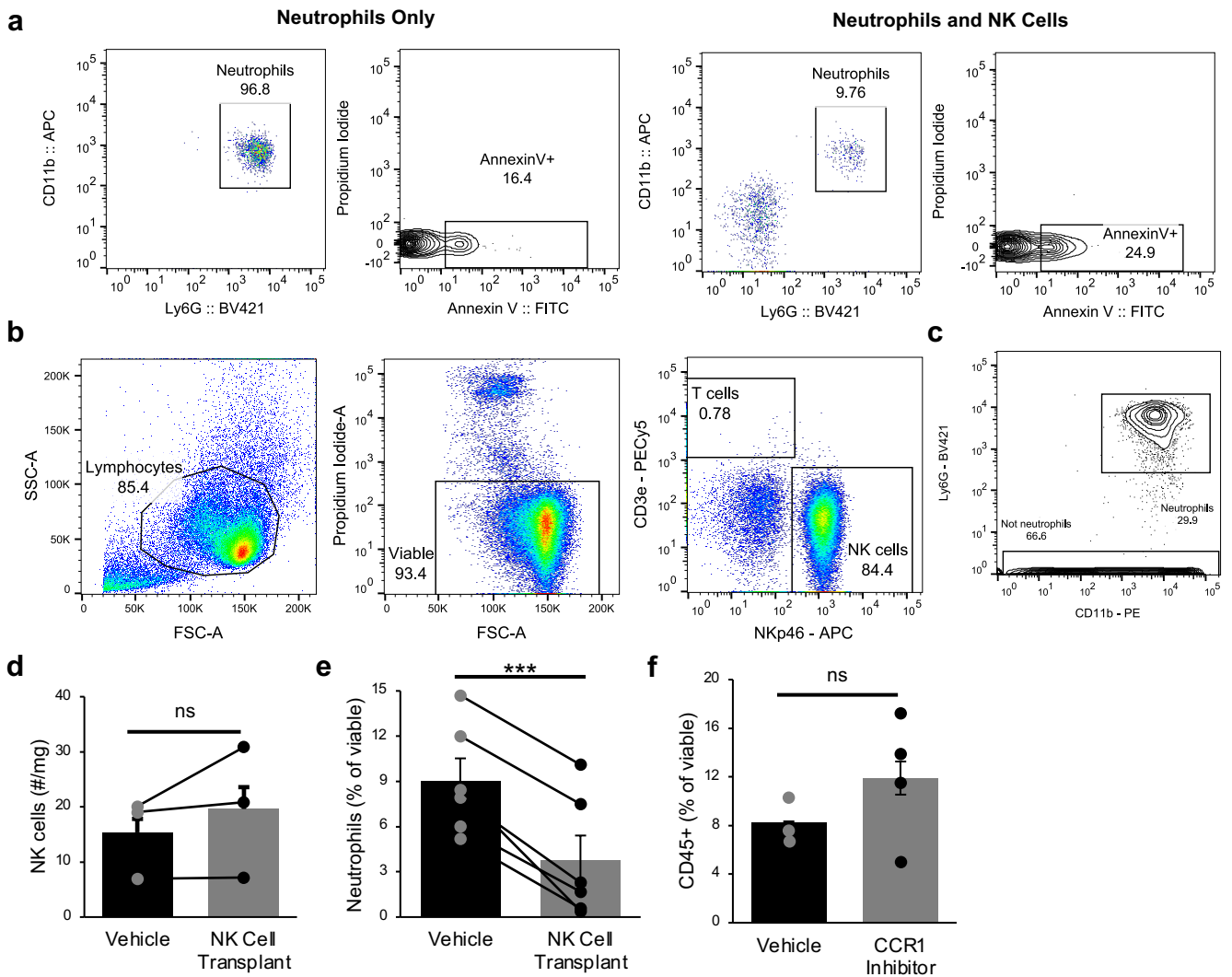
**Supplemental Figure 2. Quality control metrics for scRNA-Seq datasets and cell marker gene expression after volumetric muscle loss injuries.** (a) UMAP overlay of the number of genes detected per cell. (b) UMAP overlay of the total number of counts detected per cell. (c) UMAP colored by dataset following Seurat v3 batch correction. (d) Dot plots of marker gene expression showing different clusters of cells used for annotation. All conditions are shown (both defect sizes and all timepoints). (e) The top 8 GO terms enriched among 2mm (left) and 3mm (right) defects.



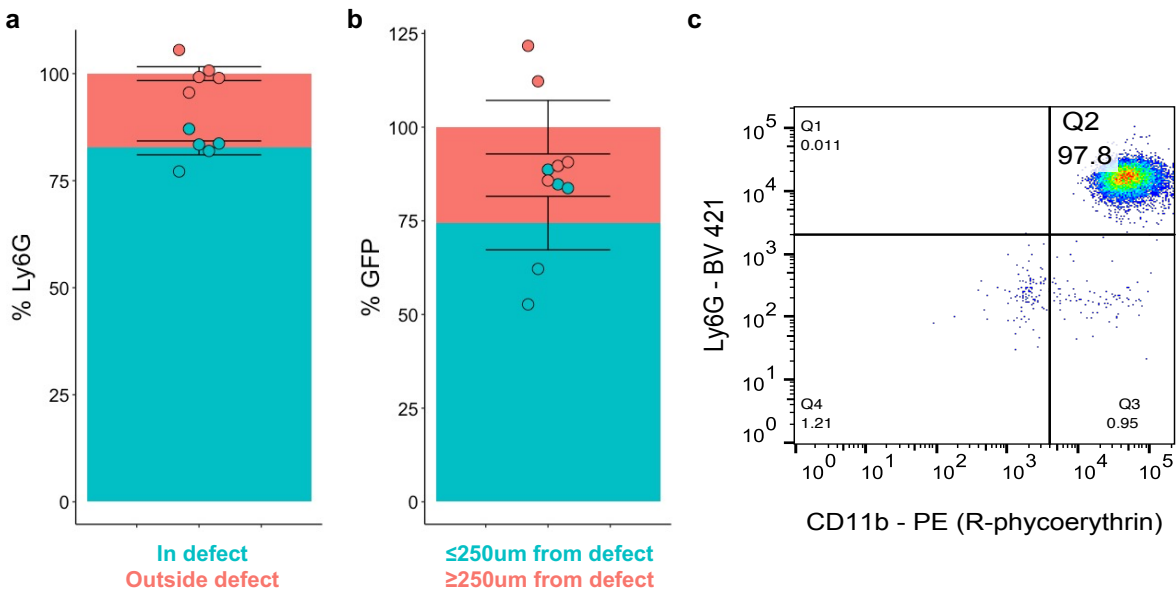
**Supplemental Figure 3. Flow cytometry verification of changes in immune cell abundances after volumetric muscle loss injuries.** (a) Representative flow cytometry scatterplots showing gating strategy for T cells and NK cells. (b) Flow cytometry quantification of CD3+ T cell abundance at 7-dpi. Bars show mean  $\pm$  SEM. No significant difference was observed by one-way ANOVA between 2mm and 3mm defects, nor after 3mm defects with PBS perfusion immediately prior to muscle harvest, though there is a trend towards more t cells in degenerative defects.  $n = 6$  muscles per group ( $N = 9$  mice). NK cell quantifications by flow cytometry are shown in Figure 2e. (c) Representative flow cytometry scatterplots showing gating strategy for neutrophils. Neutrophil abundance quantifications by flow cytometry are shown in Figure 2a.



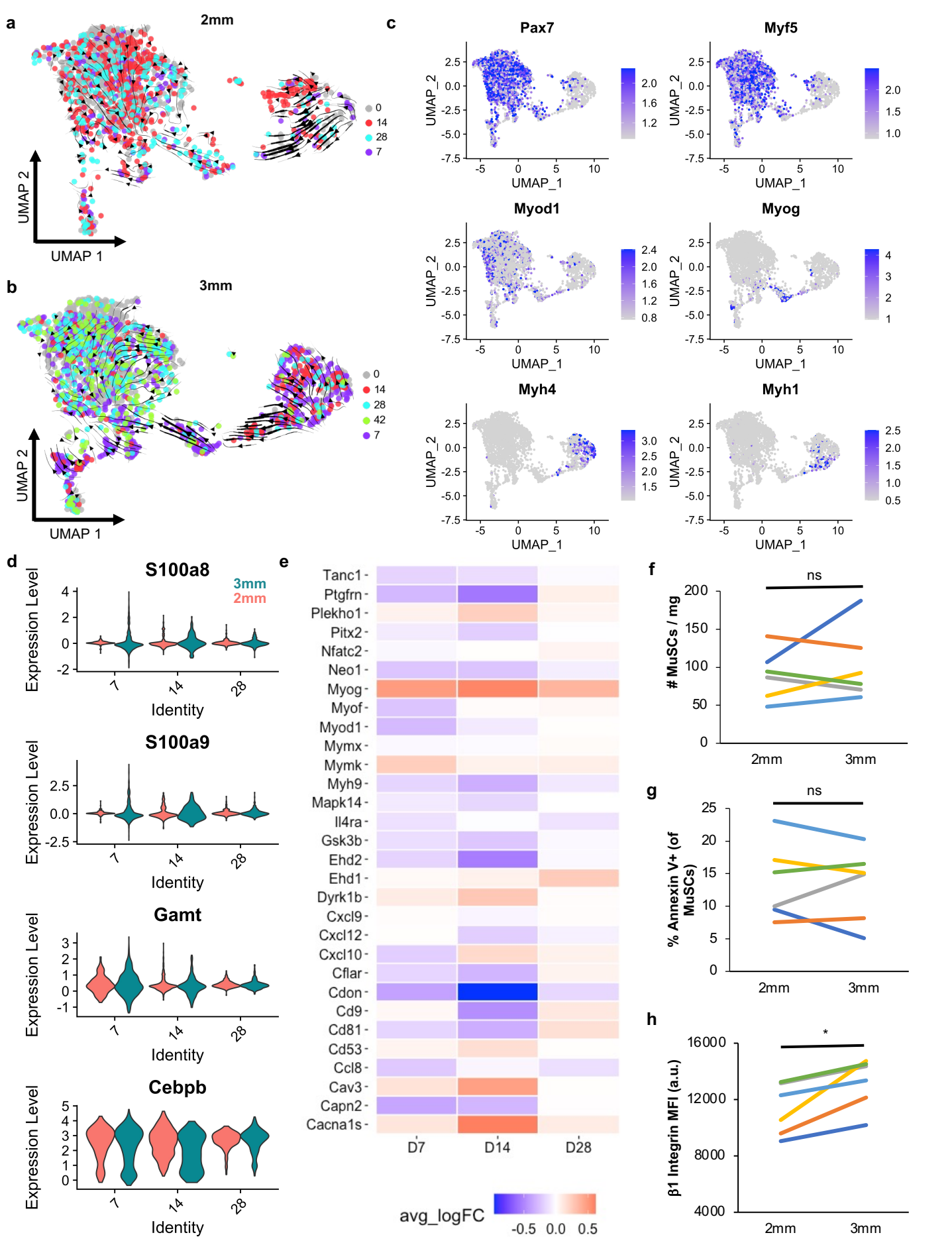
**Supplemental Figure 4. Identification and characterization of defect-infiltrating NK cells after volumetric muscle loss injuries.** (a) Expression of canonical T and NK cell marker genes overlaid onto UMAP dimensionally reduced NK/T cell cluster shows the presence of NK cells, NKT cells, and three subsets of T cells (T helper cells, cytotoxic T cells, and activated T cells). (b) Lymphocyte subtypes as a fraction of total cell population at each time point post injury in 2mm vs 3mm defects from scRNA-Seq. (c) Heatmap of differentially expressed genes across lymphocyte populations in VML defects, grouped by cell type. Tc = cytotoxic (CD8+) T cell, Th = helper (CD4+) T cell, Ta = activated T cell, NK = natural killer cell, NKT = natural killer T cell. (d) Expression of *Ccl5*, cytolytic- (*Ncr1*, *Klrk1*) and cytokine secretion- (*Klrc1*, *Ifng*, *Ltb*) associated NK cell markers in NK cells isolated from 2mm and 3mm defects.



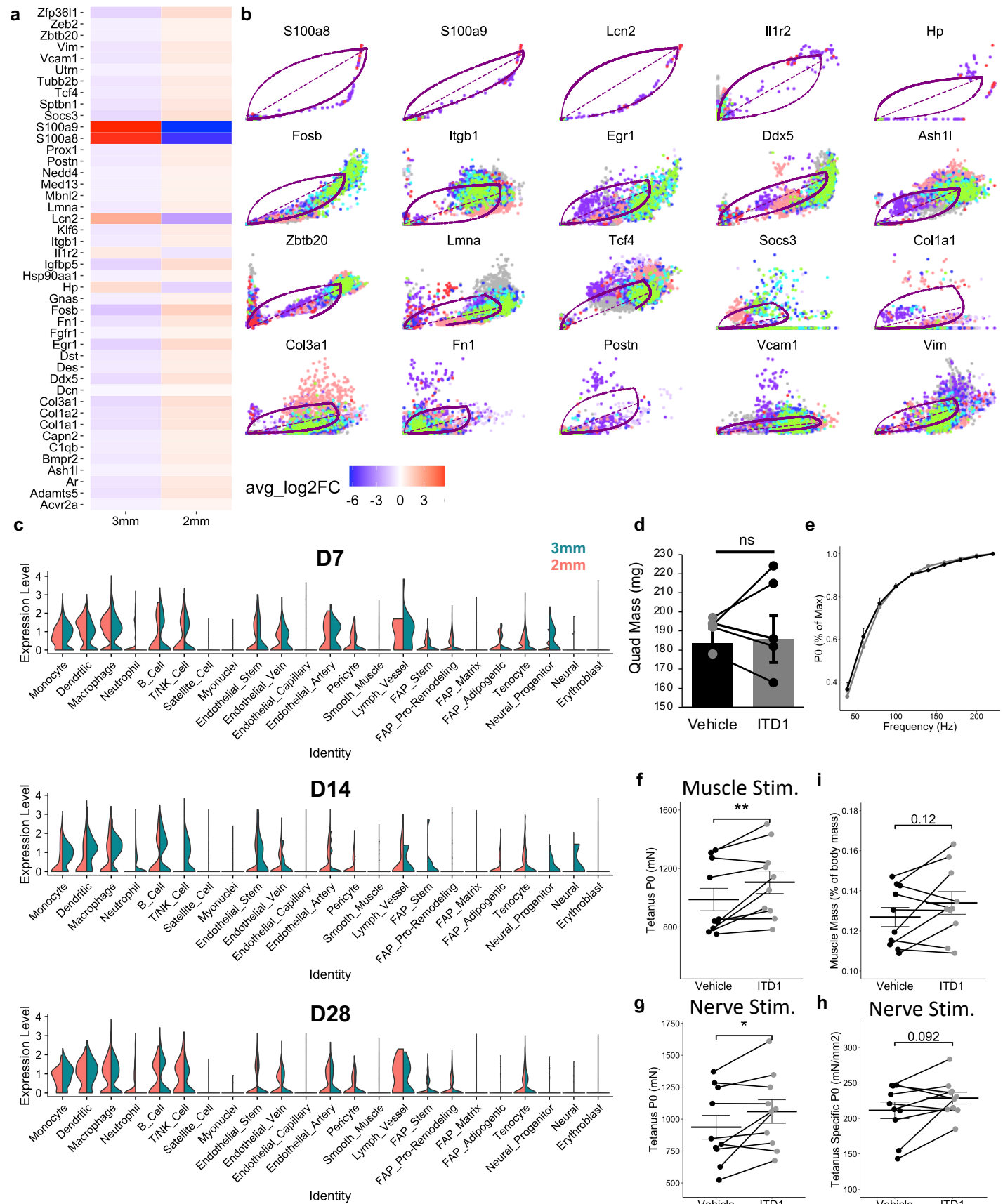
**Supplemental Figure 5. Isolation and transplantation of Natural Killer cells into muscle after volumetric muscle loss injury.** (a) Representative flow cytometry scatter plots showing gating for Annexin V co-culture staining. (b) Flow cytometry shows magnetically enriched NK cell population is ~85% pure based on NKp46 expression and 93% viable. (c) Flow cytometry gating for neutrophils and lymphocytes at 14-dpi. Cells were previously gated on PI exclusion. (d) Transplanted NK cells had cleared from the muscle by 14-dpi. Graph shows mean  $\pm$  SEM. ns denotes not significant ( $p = 0.8059$ ) by two-sided, paired t-test.  $n = 3$  muscles per group. (e) NK cell transplant into 2mm defects reduced neutrophil abundance at 14-dpi. \*\*\* $p < 0.001$  by two-sided, paired t-test. Cohen's  $d = 2.23$ .  $n = 6$  muscles ( $N = 6$  mice). Graph shows mean + standard error. (f) CCR1 inhibition resulted in a trend towards increased immune cells at 14dpi, though the 3.5 percent increase in means (8.21% in vehicle, 11.9% in CCR1i) is smaller than the increase in neutrophils as a percent of viable (6% increase), suggesting CCR1i does not largely impact abundance of other immune cell types.  $p > 0.05$  by two-sided, two-sample t-test.  $n = 3-4$  muscles ( $N = 8$  mice). Cohen's  $d = 0.89$ . Graph shows mean + SEM.



**Supplemental Figure 6. Neutrophil and muscle-stem cell derived cellular locations after volumetric muscle loss injury.** (a) Approximately 85% of Ly6G<sup>+</sup> cells are within the defect at 14-dpi. Bars show mean  $\pm$  SEM. n = 5 muscles. (b) Around 75% of GFP<sup>+</sup> myofibers are within 250 $\mu$ m of the defect at 14-dpi. n = 5 muscles. Bars show mean  $\pm$  SEM. (c) MACS-enriched neutrophil population is >95% pure by flow cytometry (Ly6G<sup>+</sup>Cd11b<sup>+</sup>).



**Supplemental Figure 7. Comparison of MuSC gene expression, apoptosis, and matrix attachment after volumetric muscle loss injuries.** (a) RNAVelocity stream plot of myogenic cells from 2mm defects across the 28-day time course. (b) RNAVelocity stream plot of myogenic cells from 3mm defects across the 42-day time course. (c) Expression overlays of canonical myogenic and myonuclei marker genes. (d) Differentially expressed genes across each condition among the MuSC scRNA-Seq cluster. (e) Heatmap of genes associated with myoblast fusion among MuSCs at different timepoints. Average fold change of each gene was calculated for MuSCs from 3mm defects in relation to MuSCs from 2mm defects at each timepoint, such that red bars indicate increased expression among MuSCs from 3mm defects and blue bars indicate reduced expression at that timepoint. (f) Number of MuSCs in quadriceps 14-dpi, quantified by flow cytometry (CD45<sup>-</sup> Ter119<sup>-</sup> CD31<sup>-</sup> Sca1<sup>-</sup> CD11b<sup>-</sup> PI<sup>-</sup> CXCR4<sup>+</sup> B1int<sup>+</sup>). n = 6 muscles per group, each mouse receiving one 2mm defect and one 3mm defect. No significant difference across defect sizes by paired t-test ( $p = 0.45$ ). Each line represents one mouse. (g) Percent of viable (PI<sup>-</sup>) MuSCs that are apoptotic (Annexin V<sup>+</sup>) 14-dpi, as determined by flow cytometry. n = 6 muscles per group, each mouse receiving one 2mm defect and one 3mm defect. No significant difference across defect sizes by paired t-test ( $p = 0.78$ ). Each line represents one mouse. (h) Integrin b1 expression is lower in MuSCs harvested from regenerative defects 14-dpi based on mean fluorescent intensity (MFI). n = 6 muscles per group. Significant difference across defect sizes by paired t-test ( $p = 0.01$ ). Each line represents one mouse.



**Supplemental Figure 8. TGF $\beta$ 1 impacts on myogenesis post VML.** (a) Average log fold change of gene expression among NicheNet predicted target genes at 7-dpi. (b) NicheNet-predicted TGF $\beta$ 1 and IL-1 signaling target genes have high likelihoods in the RNA velocity dynamical model, suggesting they play a role in governing the observed differences in MuSC fate transitions. (c) Average *Tgfb1* expression among each cell type across the time-course shows drastic upregulation primarily among macrophages and monocytes in 3mm defects. (d) ITD1 treatment had no effect on quadriceps mass at 28-dpi. (e) Force-frequency curves following treatment with ITD1 or Vehicle. Points show means, error bars show SEM. No significant difference was observed ( $p > 0.05$ ) across treatments by Wilcoxon test and holm  $p$ -value adjustment for multiple testing. (f) Impact of ITD1 on total force when the muscle was stimulated.  $**p < 0.01$  by two-sided, paired  $t$ -test.  $n = 10$  muscles,  $N = 10$  mice. (g) ITD1 treatment significantly impacted maximum tetanic force when the nerve was stimulated, (h) but it did not significantly impact specific force.  $*p < 0.05$  by two-sided, paired  $t$ -test.  $n = 10$  muscles,  $N = 10$  mice. (i) ITD1 treatment had a mild, but not significant, impact on TA muscle mass at 28-dpi.  $p = 0.12$  by two-sided, paired  $t$ -test.  $n = 12$  muscles,  $N = 12$  mice.